Opacity of an Underdense Plasma Slab due to the Parametric Instabilities of an Ultraintense Laser Pulse

J. C. Adam, A. Héron, G. Laval, and P. Mora
Centre de Physique Théorique, CNRS-Ecole Polytechnique, 91128 Palaiseau, France
(Received 19 July 1999)

The interaction of ultraintense laser beams with underdense plasma slabs has been investigated with two-dimensional particle-in-cell numerical simulations, showing a strong absorption and a correlatively low transmission. Energetic electrons in the multi-MeV range are produced. At very high intensities the plasma transparency is recovered. These results are interpreted in terms of the development of electron parametric instabilities in the self-consistently heated plasma.

PACS numbers: 52.35.Mw, 52.40.Db, 52.40.Nk, 52.65.Rr

The chirped pulse amplification of laser light has opened a new field of investigation for plasma physicists. Laser peak powers have reached up to one petawatt. By focusing this light beam, intensities larger than 10^{20} W/cm^2 are now available. A large number of such ultrahigh intensity lasers have been built to generate high energy particles for several purposes. Among them, the fast ignition of fusion targets raised great hopes by lowering the laser energy required to obtain the fuel burning and a thermonuclear gain [1]. The fast ignition principle relies upon the assumption that the oscillating electrons can be converted into a high energy particle beam which will heat the dense core of a compressed pellet.

However, several physics issues have to be examined before one is able to make a realistic assessment of the method. Among them, the propagation of the ultraintense pulse through the underdense corona is challenging. The short intense pulse has to propagate through the long coronal plasma without deviation, filamentation, and absorption. The current solution implies that a long intense prepulse will first drill a channel in the coronal plasma [2]. Once this channel formed, the following ultraintense pulse will reach more easily the dense core.

In order to define the desirable parameters of the residual plasma inside the channel, it is necessary to know how the ultraintense pulse will interact with it. This is the purpose of several experiments in which an ultraintense pulse interacts with a preformed underdense or slightly overdense plasma. In these experiments, anomalous absorption has been observed [3] as well as a strong reduction of the transmission through moderately underdense plasmas. For similar parameters, high energy electrons have been detected [4].

In this paper, the interaction of an ultraintense 1 μm laser pulse with slightly underdense plasmas will be investigated by using two-dimensional (2D) numerical particle-in-cell (PIC) simulations, and the results will be discussed in the light of theoretical calculations. The electromagnetic wave is linearly polarized with the electric field in the plane of the simulation. The temporal pulse shape is approximately Gaussian with a full width at half maximum (FWHM) of $600\omega_0^{-1}$, where $\omega_0 = 2\pi c/\lambda_0$ and $\lambda_0 = 1$ μm is the vacuum wavelength. This pulse duration is in the range corresponding to present experiments. The radial intensity profile is assumed to be Gaussian with a FWHM of $5\lambda_0$. The simulation box initially contains a plasma slab, with sharp edges normal to the direction of incidence of the laser. The slab width is $200\lambda_0$, and on each side of the plasma slab, there is a $35\lambda_0$ vacuum region. In the transverse direction, the simulation box is $73\lambda_0$ wide. There are approximatively 21 grid points per λ_0 in both directions which yield a total of 8.4×10^6 grid points. We use a total of 74×10^6 particles which gives approximatively 11 particles per grid point inside the plasma slab. The boundary conditions are periodic in the transverse direction and open in the direction of propagation. In order to avoid interaction between the simulation box and its periodic images, the particles are cooled as they cross the transverse boundary. The electron to ion mass ratio is 1/1836 and the initial temperature is 1 KeV. One run lasts 15 h on the 64 processors of a Cray/T3E.

A series of simulations have been performed with $0.1 < n/n_c < 0.4$ and $10^{16} < I_m < 5 \times 10^{20}$ W/cm^2 where n is the electron density, n_c is the critical density corresponding to λ_0, and I_m is the maximum intensity of the pulse. In this range of intensities and for 1 μm wavelength the relativistic mass factor γ of an electron oscillating in the laser field varies from 1.0 to 12.5. The transmission and the reflection coefficients were obtained by computing the outgoing flux of the Poynting vector through the simulation box boundaries, and the absorption coefficient was given by the overall energy flux balance.

Figures 1(a)–1(c) show plots of the transmission, reflection, and absorption coefficients as a function of I_m for $n/n_c = 0.1$, 0.2, and 0.4. These results show that the transmission initially decreases with I_m, becomes very low for $I_m = 10^{19}$–10^{20} W/cm^2, and eventually increases again quite abruptly. Figure 1(a) also shows that at relativistic intensities the transmission is reduced for fixed intensity and growing density. Since high intensities lead to an effective density n/γ lowered by relativistic effect,

 0031-9007/00/84(16)/3598(4)$15.00

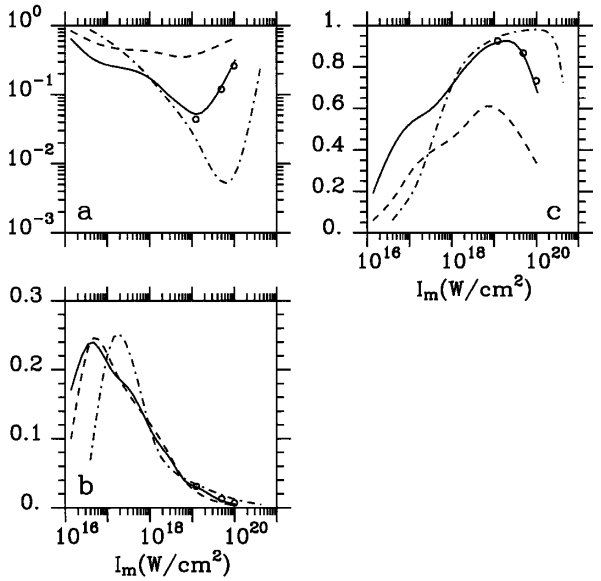

FIG. 1. The 2D PIC simulation of the interaction of a laser pulse with a plasma slab for three different densities as a function of flux. (a) is the transmission coefficient, (b) is the reflection coefficient, and (c) is the absorption rate. The dashed line is for $n/n_c = 0.1$, the solid line for $n/n_c = 0.2$, and the dash-dotted line for $n/n_c = 0.4$. The circles correspond to $n/n_c = 0.2$ and fixed ions.

one could think that this effect can explain the increase in transmission with intensity at fixed density. However, it will be shown further that this effect is not sufficient by itself to explain our data. The reflection coefficient [Fig. 1(b)] reaches 0.25 for fluxes in the 10^{17} W/cm^2 range and falls down for higher fluxes to negligible values for $I_m = 10^{20}$ W/cm^2. The absorption coefficient [Fig. 1(c)] shows a surprisingly strong energy transfer between the electromagnetic wave and the plasma in the relativistic regime $I_m = 10^{19}$–10^{20} W/cm^2, whereas, in this density range, the absorption is very low both at lower fluxes, as predicted by linear propagation theory, and for very high intensities. The results are not significantly modified if the ions are fixed, at least for $I_m > 10^{18}$ W/cm^2. This rules out the radial acceleration of ions by the ponderomotive force as the origin of the anomalous absorption in the range $I_m = 10^{19}$–10^{20} W/cm^2, as well as the creation of a hollow density channel as the origin of the transmission in the very high intensity limit.

For moderately relativistic flux ($I_m < 10^{18}$ W/cm^2) we interpret the transmission decrease as being due to the Raman-type scattering instabilities which erode the back part of the pulse [5]. Simple estimates based on a spatio-temporal calculation of the behavior of the unstable modes [5] lead to a transmission decreasing as $I_m^{-1/2}$ in the standard (Raman) regime and as $I_m^{-1/3}$ in the strongly coupled (Compton) regime. This estimate, however, neglects the plasma heating which reduces the instability growth rate, especially for lower densities. Note that in the case $n = 0.4n_c$, the transmission starts to decrease for $I_m \sim 10^{17}$ W/cm^2, while the reflection coefficient exhibits a sharp jump up to 25% when relativistic effects start to be important, allowing again Raman-like instabilities [6]. At higher intensities the reflection coefficient becomes only weakly dependent on the density.

In the fully relativistic regime, parametric instabilities cannot be studied by using the resonant weak coupling approximation. The laser wave propagation is itself nonlinear, and simple solutions are available only for circular polarization. In such a case and for a cold plasma, the stability of the solution with respect to longitudinal perturbations has been thoroughly investigated [6]. For $0.1 < n/n_c < 0.4$, the usual forward and backward branches of the Raman stimulated scattering merge into a mixed instability in which the Stokes and anti-Stokes waves are both involved. In order to explain the simulations' behavior, the very fast growth of the instability and the very low phase velocity of the plasma wave have to be taken into account. These features show that, after a few femtoseconds, wave breaking occurs for the longitudinal perturbation, leading to an efficient longitudinal heating of the electrons. This heating stabilizes the backward modes with low phase velocity. Such stabilization of the backward Raman scattering has already been observed in experiments [7], where the bursting of the reflected light was interpreted as signs of the wave breaking for the longitudinal perturbation.

In order to settle this point in a more quantitative way, the parametric instability dispersion equation that has been established for longitudinally headed plasmas [6] is solved numerically. The unperturbed electron distribution function in momentum space is assumed to be cold in the transverse direction. As regards the longitudinal velocity dependence, the distribution function is a Gaussian with a zero average momentum and a rms momentum δ in mc units which is a good approximation of the distribution functions obtained in the particle simulations. In Fig. 2(a) the maximum growth rate $\gamma_{\max}$ is plotted as a function of the intensity for $\delta = 0$, 0.5, 1, 2, 4, and 16. Also shown in Fig. 2(b) is the real part of the frequency of the plasma wave for the value of the wave number corresponding to $\gamma_{\max}$. Both curves are normalized to the laser frequency ω_0. Figure 2(a) shows that $\gamma_{\max}$ is strongly reduced by the electron heating. However, for a given value of δ Fig. 2(a) shows that the growth rate does not decrease significantly at high intensity. This shows that the heating is much more efficient in reducing the growth rate than the intensity by itself. In addition, the most unstable modes are no longer associated with the backscattering modes as k is easily reduced below 1. One also notices that for $\delta > 1$ the phase velocity is such that the longitudinal wave is strongly damped. Figure 2(b) shows that even a weak increase in the longitudinal temperature yields a significant upward shift of the real part of the plasma wave frequency which is no longer a pure plasma mode. This in turn implies a very large down-shift of the scattered light.

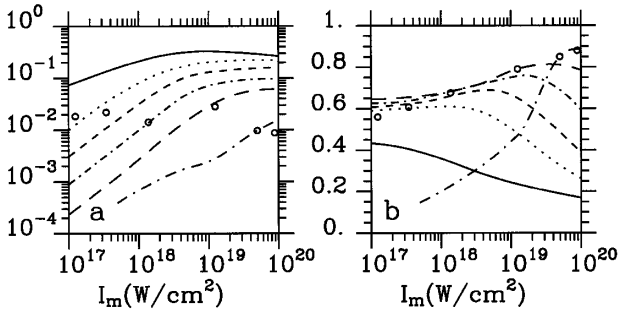

FIG. 2. Solution of 1D dispersion relation for longitudinally hot plasma for $n = 0.2n_c$. (a) is the growth rate and (b) is the real part of the frequency normalized to the laser frequency. The solid line is for $\delta = 0$, the dotted line for $\delta = 0.5$, the short dashed line for $\delta = 1$, the short dash-dotted one for $\delta = 2$, the long dashed line for $\delta = 4$, and the long dash-dotted one for $\delta = 16$. The circles correspond to the solution of the dispersion relation for the local value of δ estimated in the 2D simulations.

As a consequence in the hot plasma regime the laser pulse is forwardly scattered and absorbed by a strong stimulated Compton scattering. The circles on the plot correspond to the theoretical growth rates obtained from an estimate of δ in the 2D simulations. We attribute the large transmission rates observed at very high intensity to the very efficient plasma heating. In this regime the heating rate is fast enough to nearly stabilize the instability on a time scale significantly shorter than the pulse duration, and the back part of the pulse is then transmitted with a low absorption rate. This interpretation is supported by the examination of the evolution of the intensity profile, as it propagates through the plasma, for a wide range of intensity. At low I_m, one observes that the front of the pulse is unaffected while its back is eroded. As I_m is increased, a larger and larger fraction of the pulse is degraded until the minimum of transmission is reached. For larger values of I_m, the back of the pulse that propagates into a very hot plasma begins to be less affected by the instability and a more and more significant part of it is transmitted. This is illustrated in Fig. 3 which represents snapshots of the Poynting vector inside the plasma slab integrated in the transverse direction at different times (the time interval between snapshots is $400\omega_0^{-1}$) for two different intensities. Figure 3(a) corresponds to $I_m = 10^{18}$ W/cm^2 and $n = 0.2n_c$, for which the shape of the pulse is globally distorted as it propagates through the plasma. Figure 3(b) corresponds to $I_m = 10^{20}$ W/cm^2 and $n = 0.2n_c$, for which only the front of the pulse is eroded while the back is transmitted.

Up to now we have discussed the results on the basis of a 1D theory. However, the importance of transverse effects is clear in Fig. 4 where the distribution of the laser intensity has been plotted 420 fs after the edge of the pulse has reached the plasma slab and 300 fs later for $I_m = 10^{20}$ W/cm^2 and $n = 0.2n_c$. Initially a strong self-focusing yields a maximum intensity of more than

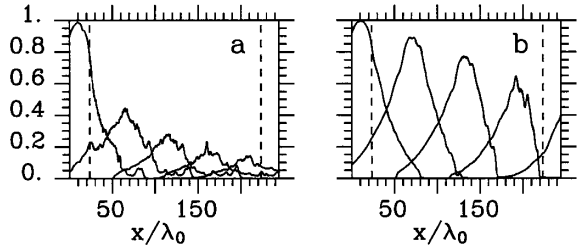

FIG. 3. Snapshots of the profile of the pulse energy as it propagates through the plasma. (a) is for $I_m = 10^{18}$ W/cm^2 and (b) is for $I_m = 10^{20}$ W/cm^2. Snapshots are plotted at time intervals of $400\omega_0^{-1}$ starting at time $600\omega_0^{-1}$ and normalized to I_m. The dotted line represents the initial limit of the plasma slab.

twice its initial value as well as filamentation of the lateral edges of the pulse. Later on, the radial structure of the pulse is severely distorted. As already noticed [9], It is seen that filamentation and strong self-focusing may occur even for such narrow beams, leading to a further increase of the maximum intensity, significantly above I_m. In addition, side scattering instabilities may play an important role. These transverse processes have to be taken into account in the explanation of the strong absorption since 1D simulations exhibit a higher transparency [10]. Transverse instability effects have been studied theoretically in the cold plasma case only [11]. It has been shown that the instability features of the 1D case extend in the transverse direction, so that instabilities with large transverse mode numbers are expected to be excited as the purely longitudinal modes. However, the growth rate is always maximum for purely longitudinal wave numbers. In the simulations, these oblique modes are found to have amplitudes lower than the parallel ones but they are responsible for the observed transverse heating which is slightly smaller than in the longitudinal direction. However, this transverse heating cannot explain by itself the larger absorption in 2D simulations. The oblique modes could also have an efficient effect on the longitudinal heating by destroying the distribution function plateau which would be formed in a short time with purely 1D longitudinal modes, avoiding

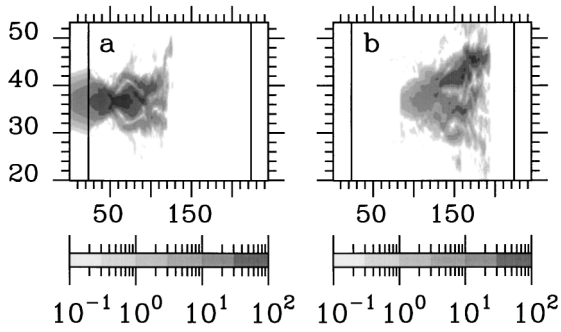

FIG. 4. Flux of the Poynting vector at time 420 fs (a) and time 720 fs (b) as a function of space for a flux of 10^{20} W/cm^2 and $n/n_c = 0.2$. Strong self-focusing as well as filamentation can be seen in (a) [8].

then a saturation of the heating mechanism and allowing them to reach very high average energies.

An interesting signature, from both the experimental and the theoretical points of view, of the existence of the instability is provided by the examination of the reflected and transmitted light spectra. Such spectra are plotted in Fig. 5 for $I_m = 10^{19}$ W/cm^2. The corresponding curves are the Fourier transforms of the purely longitudinal transmitted or reflected light obtained using a window in time of $300\omega_0^{-1}$ width. The backscattered spectrum at an early time is shown in Fig. 5(a). It shows two peaks at $0.8\omega_0$ and $0.3\omega_0$. The higher frequency peak corresponds to the cold plasma backscattering instability while the lower one results from Compton scattering on the heated plasma. At a later time [Fig. 5(b)] the peak at $0.8\omega_0$ is unchanged, while the low frequency one has decreased, which reflects the reduction of the backscattering. The persistence of the peak at $0.8\omega_0$ indicates that it is generated at the front of propagation of the pulse. Figure 5(c) shows the transmission of the front end of the pulse. It is mostly a forward scattering broad spectrum. Later in time [Fig. 5(d)] most of the transmitted energy corresponds to the incident frequency, but one can note the persistence of the forward scattered light at the same level as in Fig. 5(c). The shape of these spectra varies only weakly with the intensity; however, when the transmission is high the mode $\omega = \omega_0$ is more dominant.

In summary, PIC simulations have shown that moderately dense plasmas absorb efficiently short pulses of laser light in the relativistic regime. This anomalous absorption is linked to the excitation of strong Raman-type parametric instabilities, leading to a bulk heating of the electrons which stabilizes the backward scattering instability and leaves stimulated Compton scattering instabilities to further heat the electrons to relativistic energies. Though it is not yet possible to draw final conclusions for the conditions of fast ignition, our results indicate that the main pulse may lose energy if the preformed channel still contains a low density plasma.

We acknowledge fruitful discussions with F. Amiranoff, S. Baton, J. Fuchs, L. Gremillet, and C. Rousseaux. The computations were performed using IDRIS, the CNRS central computing facility.

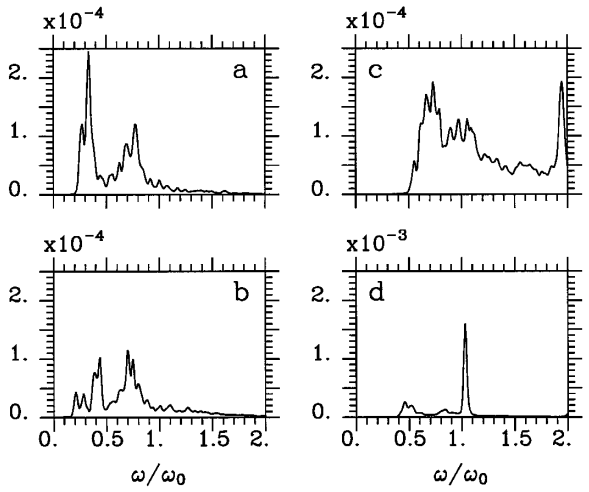

FIG. 5. Spectrum of reflected light [(a) and (b)] in arbitrary units. Spectrum of transmitted light [(c) and (d)] in arbitrary units. Note that the scale in (d) is 10 times larger than the one in (c).

[1] M. Tabak *et al.*, Phys. Plasmas **1**, 1826 (1994).
[2] M. Borghesi *et al.*, Phys. Rev. Lett. **78**, 879 (1997); J. Fuchs *et al.*, Phys. Rev. Lett. **80**, 1658 (1998).
[3] J. A. Cobble *et al.*, Phys. Plasmas **4**, 3006 (1996).
[4] G. Malka *et al.*, Phys. Rev. Lett. **79**, 2053 (1997).
[5] T. M. Antonsen, Jr. and P. Mora, Phys. Fluids B **5**, 1440 (1993).
[6] S. Guérin *et al.*, Phys. Plasmas **2**, 2807 (1995).
[7] C. A. Coverdale *et al.*, Phys. Rev. Lett. **74**, 4659 (1995); A. Modena *et al.*, Nature (London) **377**, 606 (1995).
[8] A color copy is available at http://www.cpht.polytechnique.fr/articles/heron.
[9] A. Pukhov and J. Meyer-ter-Vehn, Phys. Rev. Lett. **76**, 3975 (1996).
[10] J. C. Adam *et al.*, Phys. Rev. Lett. **78**, 4765 (1997).
[11] B. Quesnel *et al.*, Phys. Rev. Lett. **78**, 2132 (1997); A. S. Sakharov and V. I. Kirsanov, Plasma Phys. Rep. **21**, 632 (1995).